Fault Diagnosis of Gears used in Wind Turbine Powertrain

HRIDIN PRADEEP



DEPARTMENT OF MECHANICAL ENGINEERING

INDIAN INSTITUTE OF TECHNOLOGY DELHI

JUNE 2026

© Indian Institute of Technology Delhi (IITD), New Delhi, 2026

Fault Diagnosis of Gears used in Wind Turbine Powertrain

by

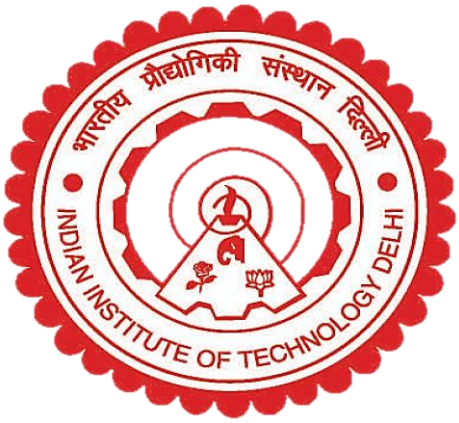
HRIDIN PRADEEP

Department of Mechanical Engineering

Submitted

in fulfilment of the requirements of the degree of DOCTOR OF PHILOSOPHY

to the



INDIAN INSTITUTE OF TECHNOLOGY DELHI

JUNE 2026

Dedicated to My Father V. N. Pradeep (Late)

My Mother Nandini Pradeep, My Sister Hridya Pradeep

and My niece Haimi Girija Hareesh

CERTIFICATE

This is to certify that the thesis entitled **FAULT DIAGNOSIS OF GEARS USED IN WIND TURBINE POWERTRAIN** submitted by Mr. HRIDIN PRADEEP to the Indian Institute of Technology Delhi for the award of the degree of Doctor of Philosophy is a bonafide record of research work carried out by him under my supervision. This thesis has been prepared in conformity with the rules and regulations of the Indian Institute of Technology Delhi. I further certify that the thesis has attained a standard required for a degree Doctor of Philosophy. The research reported and the results presented in the thesis, in full or in parts, have not been submitted to any other Institute or University for the award of any degree or diploma.

_____

Dr Ashish K Darpe
Professor
Department of Mechanical Engineering
Indian Institute of Technology Delhi
New Delhi- 110016, India

Date_____

ACKNOWLEDGEMENTS

I begin by expressing my profound gratitude to **Prof. S. P. Singh**. At a moment when I was enduring my most difficult days, his guidance and kindness arrived like a beacon of light, and I shall always remember his timely support.

My deepest appreciation goes to my supervisor, **Prof. Ashish K. Darpe**. His unwavering patience, empathy, and encouragement allowed me to rediscover confidence in myself and to recognise abilities I had doubted. The opportunities he offered—both within this project and in related research—were invaluable to my growth as a researcher and as a person.

I am equally thankful to the members of my Student Research Committee (SRC)—**Prof. J. K. Dutt, Prof. B. P. Patel, and Prof. S. V. Modak**—for their guidance, constructive criticism, and thoughtful suggestions. I also thank **Prof. K. Gupta** for his motivating words throughout my doctoral journey. The anonymous reviewers who assessed my manuscripts contributed insightful comments that greatly improved the published work; their efforts are sincerely appreciated.

My sincere appreciation goes to **IIT Delhi** and the **Ministry of Education (formerly MHRD), Government of India**, for the facilities and financial support that made this journey possible.

I owe a special debt to **Mr. K. N. Madhu**, whose father-like counsel sustained me at every step. I also thank my colleagues—**Dr. Anvesh Reddy, Dr. Pradeep Kundu, Gyan Setu, Anuj Dahiya, and Sarthak Mittal**—and my friends **Dr. Dharmender, Abhishekh Rana, N. Jayakrishnan, Akhil G. S., Dr. Hemant Praveen, Dr. Priya Bose, Soham Das, and Sriparna Roy** for their camaraderie and support.

I owe special thanks to the pillars of my life **Dr. Jinju S., Dr. Salini S., Dr. Sreejath S., Dr. Binoy B., and Greeshma Joseph** for filling my life with resilience and hope; and to my family—especially my sister **Hridya Pradeep** and my mother **Nandini Pradeep**—for their endless love and support since my earliest days. The arrival of my niece, **Haimi Girija Hareesh**, during my studies has been a source of boundless joy and inspiration. Last but not the least, I extend my sincere thanks to **Dr. Piyush Shakya, Associate Professor, Department of Mechanical Engineering IIT Madras** for the chance he has given to me to work as a post-Doc Fellow the completion of my PhD defence.

The years spent at IIT Delhi have been transformative, filled with experiences and friendships that I will cherish forever. "*Jai Hind"*

Hridin Pradeep

ABSTRACT

Wind-turbine gearboxes operate under large; fluctuating torques and harsh environmental conditions; their early-stage faults are therefore a leading cause of unexpected downtime and maintenance costs. This dissertation develops an end-to-end framework, spanning physics-based modelling, signal-level health indicator design, and data-driven classification for the detection, localisation and severity quantification of multiple, simultaneously occurring gear-mesh faults in utility-scale wind-turbine drivetrains.

The study begins with a first-principles derivation of **time-varying mesh stiffness (TVMS)**. Closed-form expressions are obtained for healthy spur meshes and then extended to seven fault classes: tooth breakage, root crack, partial chipping, pitting, uniform wear, parabolically distributed wear, and all hybrid combinations thereof. Numerical results agree to within 3 % of published benchmarks, confirming the accuracy of the formulation. The TVMS library is embedded in lumped-parameter dynamic models of (i) a parallel-axis intermediate/high-speed gearbox and (ii) a planetary low-speed stage featuring seven degrees of freedom per central member. Generalised-α and β-Newmark integration schemes yield high-fidelity input- and output-shaft torque histories for healthy, singly faulted and hybrid-faulted conditions.

Time- and frequency-domain analysis of these simulations shows that a fully broken tooth excites torsional natural modes most strongly, whereas pitting, cracking, and chipping produce progressively weaker signatures; distributed wear alone is difficult to discern without aligning, resampling, and obtaining the difference signal between healthy and faulty signals. At the planetary stage, modified Hamming transfer-path filtering shows that **the output shaft difference torque** is the most information-rich channel after carrier-speed modulation is removed.

Building on these insights, over thirty **Health indicators (HIs)** are evaluated. Classical statistical metrics (RMS, peak-to-peak, kurtosis, crest factor), higher-order moment ratios (FM4, NA4), side-band energy ratios, and newly proposed distribution-shape measures—correlation coefficients of second and fourth histogram moments (CCS, CCF) and their weighted fusion (CCSF)—exhibit monotonic, trend-able behaviour across 0–80 % crack and 0–15 bps wear severities. Crest factor is identified as the most robust single HI for localised defects, while CCSF offers linear sensitivity across the entire crack-growth range.

Finally, a physics-informed machine-learning layer is introduced. Fourteen time-domain torque features feed a suite of feed-forward neural networks: a binary classifier discriminates crack vs wear with 80–100 % accuracy, and two regression models predict severity with $R^2 = 0.998$ (crack) and 0.989 (wear). The lightweight two-hidden-layer architecture balances interpretability and real-time deployability, demonstrating that carefully selected physics-consistent features obviate the need for computationally intensive spectro-temporal transforms.

Collectively, the work delivers: (1) the first comprehensive TVMS atlas for simultaneously distributed and localised faults; (2) high-fidelity drivetrain models that capture fault-induced resonance interaction; (3) a hierarchical diagnostic toolkit—from rapid statistical alarms to neural-network decision support—capable of early, quantitative fault assessment using a single high-speed-shaft sensor. These advances pave the way for predictive-maintenance digital twins that can reduce unscheduled turbine downtime, extend component life and lower the levelized cost of renewable energy.

सारांश

पवन-टरबाइन गियरबॉक्स उच्च एवं निरंतर परिवर्तित होने वाले टॉर्क तथा कठोर पर्यावरणीय परिस्थितियों में कार्य करते हैं। परिणामस्वरूप, इनमें उत्पन्न होने वाले प्रारम्भिक चरण के दोष अप्रत्याशित डाउनटाइम तथा रखरखाव लागत में वृद्धि के प्रमुख कारणों में से एक हैं। यह शोध-प्रबंध उपयोगिता-स्तरीय पवन-टरबाइन ड्राइवट्रेन में एक साथ उत्पन्न होने वाले बहुविध गियर-मेश दोषों के पता लगाने, स्थान-निर्धारण तथा उनकी गंभीरता के परिमाणीकरण हेतु भौतिकी-आधारित मॉडलिंग, संकेत-स्तरीय स्वास्थ्य संकेतक (Health Indicators) के विकास तथा डेटा-आधारित वर्गीकरण को समाहित करते हुए एक समग्र ढाँचा प्रस्तुत करता है।

अध्ययन का प्रारम्भ समय-परिवर्ती मेश कठोरता (Time-Varying Mesh Stiffness, TVMS) के प्रथम-सिद्धांत आधारित व्युत्पादन से किया गया है। स्वस्थ स्पर गियर मेश के लिए बंद-रूप (Closed-form) समीकरण विकसित किए गए तथा बाद में उन्हें सात विभिन्न दोष श्रेणियों—दांत टूटना (Tooth Breakage), मूल दरार (Root Crack), आंशिक चिपिंग (Partial Chipping), पिटिंग (Pitting), समान घिसाव (Uniform Wear), परवलयिक रूप से वितरित घिसाव (Parabolically Distributed Wear) तथा इनके सभी संकर (Hybrid) संयोजनों—तक विस्तारित किया गया। संख्यात्मक परिणाम प्रकाशित मानकों की तुलना में 3% से कम त्रुटि के भीतर पाए गए, जिससे विकसित मॉडल की सटीकता प्रमाणित होती है। इस TVMS डेटाबेस को (i) समानांतर-अक्ष मध्यवर्ती/उच्च-गति गियरबॉक्स तथा (ii) सात स्वतंत्रता-अंशों वाले ग्रहीय निम्न-गति चरण (Planetary Low-Speed Stage) के लम्प्ड-पैरामीटर गतिशील मॉडलों में समाहित किया गया। Generalized-α तथा β-Newmark समाकलन विधियों का उपयोग करते हुए स्वस्थ, एकल-दोषयुक्त तथा संकर-दोषयुक्त स्थितियों के लिए इनपुट एवं आउटपुट शाफ्ट टॉर्क के उच्च-निष्ठा (High-Fidelity) समय-इतिहास प्राप्त किए गए।

इन अनुकरणों के समय-क्षेत्र तथा आवृत्ति-क्षेत्र विश्लेषण से यह ज्ञात हुआ कि पूर्णतः टूटा हुआ दांत (Fully Broken Tooth) मरोड़ीय प्राकृतिक आवृत्तियों (Torsional Natural Modes) को सर्वाधिक उत्तेजित करता है, जबकि पिटिंग, दरार तथा चिपिंग अपेक्षाकृत कमजोर संकेत उत्पन्न करते हैं। दूसरी ओर, वितरित घिसाव (Distributed Wear) को केवल स्वस्थ एवं दोषयुक्त संकेतों के संरेखण (Alignment), पुनः-नमूनाकरण (Resampling) तथा उनके अंतर-संकेत (Difference Signal) के विश्लेषण द्वारा ही स्पष्ट रूप से पहचाना जा सकता है। ग्रहीय चरण में संशोधित हैमिंग ट्रांसफर-पाथ फिल्टरिंग (Modified Hamming Transfer-Path Filtering) से यह प्रदर्शित हुआ कि वाहक गति

(Carrier-Speed) मापांक प्रभाव को हटाने के पश्चात आउटपुट शाफ्ट का अंतर टॉर्क सर्वाधिक सूचना-समृद्ध संकेत चैनल है।

इन निष्कर्षों के आधार पर तीस से अधिक स्वास्थ्य संकेतकों (Health Indicators) का मूल्यांकन किया गया। पारंपरिक सांख्यिकीय मापदंडों—RMS, पीक-टू-पीक, कर्टोसिस तथा क्रेस्ट फैक्टर—के साथ-साथ उच्च-कोटि आघूर्ण अनुपात (FM4, NA4), साइड-बैंड ऊर्जा अनुपात तथा नव-प्रस्तावित वितरण-आकृति आधारित मापदंड—द्वितीय एवं चतुर्थ हिस्टोग्राम आघूर्णों के सहसंबंध गुणांक (CCS, CCF) तथा उनके भारित संयोजन (CCSF)—का अध्ययन किया गया। इन सभी ने 0–80% दरार तथा 0–15 बेसिस-पॉइंट घिसाव गंभीरता के बीच एकरूपी (Monotonic) एवं प्रवृत्ति-अनुगामी (Trendable) व्यवहार प्रदर्शित किया। परिणामों से ज्ञात हुआ कि स्थानीयकृत दोषों के लिए क्रेस्ट फैक्टर सर्वाधिक सुदृढ़ एकल स्वास्थ्य संकेतक है, जबकि CCSF सम्पूर्ण दरार-वृद्धि सीमा में लगभग रैखिक संवेदनशीलता प्रदान करता है।

अंततः, एक भौतिकी-सूचित मशीन लर्निंग (Physics-Informed Machine Learning) स्तर विकसित किया गया। चौदह समय-क्षेत्र आधारित टॉर्क विशेषताओं (Torque Features) का उपयोग करते हुए फीड-फॉरवर्ड कृत्रिम तंत्रिका नेटवर्कों (Feed-Forward Neural Networks) का एक समूह विकसित किया गया। इनमें एक द्विआधारी वर्गीकारक (Binary Classifier) दरार एवं घिसाव दोषों के बीच 80–100% शुद्धता के साथ भेद कर सकता है, जबकि दो प्रतिगमन मॉडल दोष की गंभीरता का अनुमान क्रमशः R^2 = 0.998 (दरार) तथा R^2 = 0.989 (घिसाव) की सटीकता से प्रदान करते हैं। दो गुप्त-स्तरों (Two Hidden Layers) वाली हल्की संरचना व्याख्येयता (Interpretability) तथा वास्तविक-समय कार्यान्वयन (Real-Time Deployability) के मध्य संतुलन स्थापित करती है और यह प्रदर्शित करती है कि सावधानीपूर्वक चयनित भौतिकी-संगत विशेषताएँ जटिल स्पेक्ट्रो-टेम्पोरल रूपांतरणों की आवश्यकता को समाप्त कर सकती हैं।

सामूहिक रूप से यह शोध निम्नलिखित प्रमुख योगदान प्रदान करता है: (1) वितरित एवं स्थानीयकृत दोषों के समवर्ती प्रभावों के लिए पहला व्यापक TVMS एटलस; (2) दोष-प्रेरित अनुनाद अंतःक्रियाओं (Fault-Induced Resonance Interactions) को अभिव्यक्त करने में सक्षम उच्च-निष्ठा ड्राइवट्रेन मॉडल; तथा (3) त्वरित सांख्यिकीय चेतावनियों से लेकर तंत्रिका-नेटवर्क आधारित निर्णय समर्थन तक विस्तृत एक पदानुक्रमित निदान उपकरण-संग्रह, जो केवल एक उच्च-गति शाफ्ट सेंसर का उपयोग करके प्रारम्भिक एवं मात्रात्मक दोष मूल्यांकन करने में सक्षम है। ये उपलब्धियाँ पूर्वानुमानित अनुरक्षण (Predictive Maintenance) आधारित डिजिटल ट्विन प्रणालियों के विकास का मार्ग प्रशस्त करती हैं, जो पवन-

टरबाइन के अनियोजित डाउनटाइम को कम करने, घटकों की सेवा आयु बढ़ाने तथा नवीकरणीय ऊर्जा की समतुल्यीकृत लागत (Levelized Cost of Energy) को घटाने में महत्वपूर्ण योगदान दे सकती हैं।

Table of Contents

List of Figures ..... **xii**
List of Tables ..... **xxii**
List of Abbreviations ..... **xxiii**
List of Nomenclature ..... **xxv**
Chapter 1 Introduction 1
1.1 Research Motivation 1
1.2 Background 2
1.3 Structure of Planetary Gearbox 6
1.4 Fault Modes in Planetary Gears 7
1.5 Scope of Study 9
1.6 Organization of Thesis 10
Chapter 2 Literature Review 14
2.1 Wind Turbine Failure Analysis 14
2.2 Failure Modes of Gears 15
2.3 Dynamic Modelling of Wind turbine powertrain and its components 21
2.4 Dynamic Modelling of Gears 25
2.5 Fault Diagnosis of Planetary Gear box in wind turbine 30
2.6 Health Indicators for Fault Diagnosis 48
2.7 Intelligent Fault Diagnosis of Wind Turbine Gears 53
2.8 Concluding Remarks from Literature Review 59
2.9 Research Gaps 60
2.10 Objectives of the Work 61
Chapter 3 Mathematical Modelling of Gear Faults 63
3.1 Introduction 63
3.2 TVMS estimation of sound external-external gear pair 63
3.3 TVMS Estimation of a Sound External-Internal Gear Pair 79
3.4 Mesh Stiffness Estimation of External Gear with a Broken Tooth 84
3.5 Estimation of Mesh Stiffness of a pinion with a chipped Tooth 85
3.6 Mesh Stiffness Estimation of Pinion with a Cracked Tooth 88

3.7 Estimation of gear mesh stiffness of pinion with pitting fault 96
3.8 Estimation of gear mesh stiffness of pinion with wear fault 100
3.9 Modelling of the Occurrence of Hybrid Faults on a Gear 110
3.10 Concluding Remarks 120
Chapter 4 Dynamic Modelling of Wind turbine Gear stages 123
4.1 Introduction 123
4.2 Dynamic Modelling of Parallel axis Gear boxes considering torsional degrees of freedom 123
4.3 Torque responses from sound parallel axis gearbox using torsional degree of freedom model 127
4.4 Torque responses from a parallel axis gearbox with a broken tooth on pinion 129
4.5 Torque response from a parallel axis gear box with chipped tooth fault on pinion 134
4.6 Torque responses from a parallel axis gearbox with cracked tooth fault on pinion 136
4.7 Torque responses from a parallel axis gear box with a pitted tooth fault pinion 141
4.8 Torque responses form a parallel axis gearbox with wear fault on pinion 144
4.9 Torque responses from a parallel axis gearbox with hybrid tooth fault on pinion 150
4.10 Dynamic Modelling of Planetary Gear box using torsional degrees of freedom model 188
4.11 Torque responses from planetary gear system with crack on the sun gear .. 192
4.12 Dynamic Simulation of planetary gear stage using lumped parameter model 195
4.13 Concluding Remarks 205
Chapter 5 Dynamic Modeling of Wind turbine Powertrain 208
5.1 Introduction 208
5.2 Wind Turbine System Description 209
5.3 Wind turbine Powertrain Dynamic Model 210
5.4 Torque Responses from a healthy wind turbine 214
5.5 Torque response from chipped tooth fault on high-speed Stage..... 217
5.6 Fault Diagnosis using Difference Signals 220

5.7 Concluding Remarks 224
Chapter 6 Fault Diagnosis 226
6.1 Introduction 226
6.2 Health Indicators for Parallel axis Gearbox 226
6.3 Health Indictors for Planetary Gearbox 232
6.4 Health Indicator based on Torque Data Distribution 236
6.5 Neural-network framework for automated defect classification and severity quantification 240
6.6 Concluding Remarks 243
Chapter 7 Conclusions and Scope for Future Work 245
7.1 Consolidated Conclusions 245
7.2 Significant Research Contributions 246
7.3 Scope for Future Work 247
References 250
Appendix 269
List of Publications 270
Biodata 271

List of Figures

Figure 1.1 Different types of gears 2
Figure 1.2: Components of Wind turbine powerplant (Image Source [1]) 4
Figure 1.3: Failure frequency versus downtime per failure for wind turbines (Image source [4]) 5
Figure 1.4: Components of a planetary gearbox 6
Figure 1.5: Typical Faults associated with Gears [9] 8
Figure 1.6: Failure Statistics of wind turbine gears [10] 9
Figure 2.1: Failure statistics of wind turbine powerplant [11] 15
Figure 2.2: Transfer paths (a) from ring-planet mesh point to sensor A3 (b) from sun planet mesh point to sensor A5 (Image source [68]) 35
Figure 2.3: Sample of vibration response measured from an inhouse test rig using an accelerometer 38
Figure 3.1: Meshing of an external-external gear pair depicted through their contact and locus circles 64
Figure 3.2: Force acting on a gear tooth 67
Figure 3.3: Schematic for determining distance from tooth central line to the point on which the force is acting 69
Figure 3.4: Schematic for determining distance from tooth base circle to the point on which the force is acting 70
Figure 3.5: Schematic for estimation of lateral span from any arbitrary point from the tooth base circle. 72
Figure 3.6: Schematic for determination of location of any arbitrary point from the base circle. 72
Figure 3.7: Time varying gear mesh stiffness of a healthy gear pair system with details taken from [32] 80
Figure 3.8: Time varying mesh stiffness of a healthy gear pair, which has been replicated (Image source: [32]) 80
Figure 3.9: Time varying gear mesh stiffness of an external-internal gear pair 83
Figure 3.10: Time varying gear mesh stiffness of external internal gear pair (Image source: [31]) 83
Figure 3.11: Spur gear with a broken tooth 84

Figure 3.12: TVMS of a gear pair for one rotation of pinion with a broken tooth on pinion.....85
Figure 3.13: Schematic of gear tooth with chipping fault 87
Figure 3.14: TVMS of a gear pair with chipped tooth fault on pinion (a = 50 mm, b = 30 mm).....88
Figure 3.15: Variation of TVMS with increase in chip size parameter along the gear face width (variation of 'b', with a = 50 mm). 89
Figure 3.16: Variation of TVMS with increase in chip size parameter along the gear tooth height (variation of 'a', with b = 30 mm). 89
Figure 3.17: The cracked tooth model for case 1. 91
Figure 3.18: The cracked tooth model for case 2. 92
Figure 3.19: The cracked tooth model for case 3. 93
Figure 3.20: The cracked tooth model for case 4. 94
Figure 3.21: TVMS of gear pair with 20% crack on pinion. 95
Figure 3.22: Variation of TVMS with increasing crack fault severity. 96
Figure 3.23: Tooth section of spur gear with a single pit (Image source: [36]) 97
Figure 3.24: TVMS of gear pair with 20% pitting on pinion teeth. 99
Figure 3.25: Variation of TVMS with increasing fault severity level on pinion. 99
Figure 3.26: TVMS for one full rotation of pinion for the gear pair given in Table 3.2. 102
Figure 3.27: TVMS plot for one full rotation of pinion with a wear severity of 80 bps on the 5th tooth of the pinion. 103
Figure 3.28: Variation of TVMS with increase in wear severity level for a pinion with constant wear depth on single tooth. 103
Figure 3.29: Variation of wear depth along tooth profile (Image source: [31]).....104
Figure 3.30: Variation of wear depth along the tooth profile (Image source: [102]). 105
Figure 3.31: Wear depth as a function of tooth contact angle. 105
Figure 3.32: Curve fitting of equation (3.104) for wear depth along the tooth profile. .106
Figure 3.33: Instantaneous pressure angle at any point of contact on gear tooth. 106
Figure 3.34: TVMS plot for one full rotation of pinion with a maximum wear depth of 80 bps on the 5th tooth of the pinion. 108
Figure 3.35: Variation of TVMS with increase in wear severity level for a pinion with varying wear depth on single tooth. 109

Figure 3.36: TVMS for one full rotation of the pinion with a wear depth corresponding to 20bps on all teeth of the pinion.....109
Figure 3.37: Comparison of wear depth estimation with tooth having full profile wear to the same value as maximum wear depth (a)20 bps (b)60 bps (c)100 bps (d)200 bps. ...112
Figure 3.38: TVMS of gear pair with a broken tooth and chipped tooth on the pinion. 112
Figure 3.39: TVMS of a gear pair with a broken tooth and 40% crack on the pinion..114
Figure 3.40: TVMS of a gear pair with a broken tooth and 20% pitting on the pinion. 114
Figure 3.41: TVMS of a gear pair with a broken tooth and a worn tooth on the pinion. 115
Figure 3.42: TVMS of a gear with a chipped tooth and a cracked tooth.....116
Figure 3.43: TVMS of a gear pair with a chipped tooth and a pitting tooth on pinion. 116
Figure 3.44: TVMS of a gear with chipped tooth and worn tooth fault on pinion. 118
Figure 3.45: TVMS of a gear pair having crack and pitting fault on the pinion. 118
Figure 3.46: TVMS of gear with a cracked tooth fault and wear tooth fault.....119
Figure 3.47: TVMS of a gear pair with pitting and wear fault on pinion.....120
Figure 4.1: Schematic of parallel axis gear box. (a) System components for dynamic model construction (b)Gear pair mesh with tooth modelled as a linear spring.....124
Figure 4.2: Mode shapes and corresponding natural frequencies of gear pair.....129
Figure 4.3: Input shaft torque response of a healthy gear system in time domain. 130
Figure 4.4: Input shaft torque response of a healthy gear system in frequency domain. 131
Figure 4.5: Output shaft torque response of a healthy gear in time domain.....131
Figure 4.6: Output shaft torque response in frequency domain.....132
Figure 4.7: Torque responses from gear pair with a broken pinion tooth (a) Input shaft torque in time domain (b) Output shaft torque in time domain (c) Input shaft torque in frequency domain (d) Output shaft torque in frequency domain. 133
Figure 4.8: Comparison of difference signal between healthy and broken tooth responses in time domain (a) Input shaft torque (b) Output shaft torque 133
Figure 4.9: Torque responses of a gear pair with chipped tooth fault on pinion (a) Input shaft torque in time domain, (b) Output shaft torque in time domain, (c) Input shaft torque in frequency domain, (d) Output shaft torque in frequency domain.....135

Figure 4.10: Comparison of time domain responses of (a) Input shaft torque (b) Output shaft torque. **135**
Figure 4.11: Difference torque responses in time domain (a) Input torque (b) Output torque **136**
Figure 4.12: Input shaft torque response in time domain **137**
Figure 4.13: Input shaft torque response in frequency domain. **137**
Figure 4.14: Comparison of input shaft torques in time domain between healthy and gear pair with 40% cracked tooth on pinion. **138**
Figure 4.15: Output shaft torque response in time domain. **139**
Figure 4.16: Output shaft torque in frequency domain. **139**
Figure 4.17: Comparison of output shaft torque response in time domain for healthy and pinion with 40% crack. **140**
Figure 4.18: Difference torque response in time domain for input shaft. **140**
Figure 4.19: Difference torque response signal in time domain for output shaft. **141**
Figure 4.20: Torque response from gear pair with a maximum crack severity of 1000bps on one tooth of pinion (a) Input shaft torque in time domain, (b) Output shaft torque in time domain, (c) Input shaft torque in frequency domain, (d) Output shaft torque in frequency domain **142**
Figure 4.21: Comparison of gear pair torque responses of healthy and pinion with 20% tooth pitting area (a) Input shaft torque, (b) Output shaft torque. **142**
Figure 4.22: Difference torque response in time domain for (a) Input shaft, (b) Output shaft **143**
Figure 4.23: Torque response from gear pair with a maximum crack severity of 1000bps on one tooth of pinion (a) Input shaft torque in time domain, (b) Output shaft torque in time domain, (c) Input shaft torque in frequency domain, (d) Output shaft torque in frequency domain **145**
Figure 4.24: Comparison of torque responses in time domain (a) Input shaft torque response, (b) Output shaft torque response. **145**
Figure 4.25: Difference torque responses in time domain for (a) Input shaft, (b) Output shaft **147**
Figure 4.26: Torque response from gear pair with a maximum crack severity of 1000 bps on all tooth on pinion (a) Input shaft torque in time domain, (b) Output shaft torque in time domain, (c) Input shaft torque in frequency domain, (d) Output shaft torque in frequency domain **148**

Figure 4.27: Comparison of torque responses in time domain for gear system with wear on all pinion tooth (a) Input shaft torque response, (b) Output shaft torque response.148
Figure 4.28: Difference torque response in time domain for a gear pair with wear on all teeth of pinion (a) Input shaft, (b) Output shaft torque. 149
Figure 4.29: Torque response from gear pair with hybrid fault of broken tooth and chipped tooth fault on the pinion, (a) Input shaft torque in the time domain, (b) Output shaft torque in time domain, (c) Input shaft torque in frequency domain, (d) Output shaft torque in frequency domain. 152
Figure 4.30: Comparison of torque responses in time domain for gear system with a broken tooth and chipped tooth fault on the pinion, (a) Input shaft torque response, (b) Output shaft torque response. 153
Figure 4.31: Difference torque response in time domain for a gear pair with a broken tooth and chipped tooth fault on the pinion, (a) Input shaft, (b) Output shaft. 154
Figure 4.32: Torque response from gear pair with hybrid fault of broken and cracked tooth fault on the pinion, (a) Input shaft torque in time domain, (b) Output shaft torque in frequency domain. 155
Figure 4.33: Comparison of torque responses in time domain for gear system with a broken tooth and cracked tooth fault on the pinion, (a) Input shaft torque, (b) Output shaft torque.....155
Figure 4.34: Difference torque response in time domain for a gear pair with a broken tooth and cracked tooth fault on the pinion (a) Input shaft, (b) Output shaft. 156
Figure 4.35: Torque responses from gear pair with hybrid fault of broken tooth and pitted tooth on the pinion, (a) Input shaft torque in time domain, (b) Output shaft torque in time domain, (c) Input shaft torque in frequency domain, (d) Output shaft torque in frequency domain. 158
Figure 4.36: Comparison of torque responses in time domain for a gear system with a broken and pitted tooth on the pinion, (a) Input shaft torque, (b) Output shaft torque. 159
Figure 4.37: Difference torque response in time domain for a gear pair with a broken tooth and pitted tooth on the pinion, (a) Input shaft, (b) Output shaft. 160
Figure 4.38: Input shaft torque response from gear pair with a hybrid fault of broken tooth and wear on single tooth of the pinion in time domain.....161
Figure 4.39: Input shaft torque response from gear pair with a hybrid fault of broken tooth and wear on single tooth of the pinion in frequency domain. 161

Figure 4.40: Output shaft torque response from gear pair with a hybrid fault of broken tooth and wear on single tooth of the pinion in time domain.....162
Figure 4.41: Output shaft torque response from gear pair with a hybrid fault of broken tooth and wear on single tooth of the pinion in frequency domain. 162
Figure 4.42: Comparison of input shaft torque responses in time domain for a gear pair with a broken and wear on single tooth on the pinion. 163
Figure 4.43: Comparison of output shaft torque responses in time domain for a gear pair with a broken and wear on single tooth of the pinion. 163
Figure 4.44: Input shaft difference torque response in time domain for a gear pair with a broken tooth and wear on single tooth of pinion 164
Figure 4.45: Output shaft difference torque response in time domain for a gear pair with a broken tooth and wear on single tooth of pinion.....164
Figure 4.46: Torque responses from gear pair with hybrid fault of chipped tooth and cracked tooth on the pinion, (a) Input shaft torque in time domain, (b) Output shaft torque in time domain, (c) Input shaft torque in frequency domain, (d) Output shaft torque in frequency domain.....165
Figure 4.47: Comparison of torque responses in time domain for a gear system with chipped and cracked tooth fault on the pinion, (a) Input shaft, (b) Output shaft. 166
Figure 4.48: Difference torque response in time domain for a gear pair with chipped and cracked tooth fault on the pinion, (a) Input shaft torque, (b) Output shaft torque. 167
Figure 4.49: Torque responses from gear pair with hybrid fault of chipped tooth and pitted tooth on the pinion, (a) Input shaft torque in time domain, (b) Output shaft torque in time domain, (c) Input shaft torque in frequency domain, (d) Output shaft torque in frequency domain.....168
Figure 4.50: Comparison of torque responses in time domain for a gear system with chipped and pitted tooth fault on the pinion, (a) Input shaft, (b) Output shaft.....169
Figure 4.51: Difference torque response in time domain for a gear pair with chipped and cracked tooth fault on the pinion, (a) Input shaft torque, (b) Output shaft torque 170
Figure 4.52: Input shaft torque response from gear pair with a hybrid fault of chipped tooth and wear on single tooth of the pinion in time domain.....172
Figure 4.53: Input shaft torque response from gear pair with a hybrid fault of chipped tooth and wear on single tooth of the pinion in frequency domain. 172

Figure 4.54: Output shaft torque response from gear pair with a hybrid fault of chipped tooth and wear on single tooth of the pinion in time domain.....173
Figure 4.55: Output shaft torque response from gear pair with a hybrid fault of chipped tooth and wear on single tooth of the pinion in frequency domain. 173
Figure 4.56: Comparison of input shaft torque responses in time domain for a gear pair with a tooth chip and wear on single and separate tooth on the pinion.....174
Figure 4.57: Comparison of output shaft torque responses in time domain for a gear pair with a tooth chip and wear on single and separate tooth on the pinion.....174
Figure 4.58: Input shaft difference torque response in time domain for a gear pair with a tooth chip and wear on single tooth of pinion 175
Figure 4.59: Output shaft difference torque response in time domain for a gear pair with a tooth chip and wear on single tooth of pinion.....175
Figure 4.60: Torque responses from gear pair with hybrid fault of cracked tooth and pitted tooth on the pinion, (a) Input shaft torque in time domain, (b) Output shaft torque in time domain, (c) Input shaft torque in frequency domain, (d) Output shaft torque in frequency domain.....176
Figure 4.61: Comparison of torque responses in time domain for a gear system with cracked and pitted tooth fault on the pinion, (a) Input shaft, (b) Output shaft.....177
Figure 4.62: Difference torque response in time domain for a gear pair with cracked and pitted tooth fault on the pinion, (a) Input shaft torque, (b) Output shaft torque...178
Figure 4.63: Input shaft torque response from gear pair with a hybrid fault of cracked tooth and wear on single tooth of the pinion in time domain.....179
Figure 4.64: Input shaft torque response from gear pair with a hybrid fault of cracked tooth and wear on single tooth of the pinion in frequency domain. 179
Figure 4.65: Output shaft torque response from gear pair with a hybrid fault of cracked tooth and wear on single tooth of the pinion in time domain.....180
Figure 4.66: Output shaft torque response from gear pair with a hybrid fault of cracked tooth and wear on single tooth of the pinion in frequency domain. 180
Figure 4.67: Comparison of input shaft torque responses in time domain for a gear pair with a tooth crack and wear on single and separate tooth on the pinion. 181
Figure 4.68: Comparison of output shaft torque responses in time domain for a gear pair with a tooth crack and wear on single and separate tooth on the pinion. 181
Figure 4.69: Input shaft difference torque response in time domain for a gear pair with a tooth crack and wear on single tooth of pinion 182

Figure 4.70: Output shaft difference torque response in time domain for a gear pair with a tooth crack and wear on single tooth of pinion.....182
Figure 4.71: Input shaft torque response from gear pair with a hybrid fault of pitted tooth and wear on single tooth of the pinion in time domain.....184
Figure 4.72: Input shaft torque response from gear pair with a hybrid fault of pitted tooth and wear on single tooth of the pinion in frequency domain. 184
Figure 4.73: Output shaft torque response from gear pair with a hybrid fault of pitted tooth and wear on single tooth of the pinion in time domain.....185
Figure 4.74: Output shaft torque response from gear pair with a hybrid fault of pitted tooth and wear on single tooth of the pinion in frequency domain. 185
Figure 4.75: Comparison of input shaft torque responses in time domain for a gear pair with pitting and wear on single and separate tooth on the pinion. 186
Figure 4.76: Comparison of output shaft torque responses in time domain for a gear pair with pitting and wear on single and separate tooth on the pinion. 186
Figure 4.77: Input shaft difference torque response in time domain for a gear pair with pitting and wear on single tooth of pinion 187
Figure 4.78: Output shaft difference torque response in time domain for a gear pair with pitting and wear on single tooth of pinion.....187
Figure 4.79: Planetary gear stage (a) Schematic (b) Multibody representation of planetary gearbox. 188
Figure 4.80: Input shaft torque response for different crack (fault) severity levels on the sun gear of the planetary gearbox. 193
Figure 4.81: Input shaft difference torque responses for different crack severity levels on the sun gear of the planetary gearbox.....194
Figure 4.82: Output shaft torque response for different crack (fault) severity levels on the sun gear of the planetary gearbox. 195
Figure 4.83: Output shaft difference torque response in the form of a waterfall diagram with different crack severity levels 195
Figure 4.84: Gear mesh model of two external gears in contact 198
Figure 4.85: Response spectrums in time and frequency domain; (a) Healthy gear-pair, (b) Gear pair with a crack on sun gear, (c) Gear pair with a broken tooth on sun gear; (d) Gear pair with both crack and broken tooth on the sun gear 201

Figure 4.86: Difference signal obtained from dynamic modelling of in time and frequency domain; (a) Gear pair with a crack on sun gear, (b) Gear pair with a broken tooth on sun gear, (c) Gear pair with both crack and broken tooth on the sun gear 204
Figure 5.1: Components of Wind turbine Power train [10].....208
Figure 5.2: Dynamic model of a wind turbine powertrain.....210
Figure 5.3: Torque response from the low-speed shaft of wind turbine.....215
Figure 5.4: Torque response from intermediate speed shaft of wind turbine.....216
Figure 5.5: Torque response from high-speed shaft of wind turbine 217
Figure 5.6: Dynamic model of a wind turbine powertrain with chipped tooth fault on high-speed gear stage.....217
Figure 5.7: Low-speed shaft torque in time domain for (a) One rotation of the rotor, (b) One rotation of the generator 219
Figure 5.8: Intermediate-speed shaft torque in time domain for (a) One rotation of the rotor, (b) One rotation of the generator.....219
Figure 5.9: High-speed shaft torque in time domain for (a) One rotation of the rotor, (b) One rotation of the generator 220
Figure 5.10: Low speed shaft difference torque signal in time domain for, (a) One rotation of rotor, (b) One rotation of generator.....221
Figure 5.11: Intermediate shaft difference torque signal in time domain for, (a) One rotation of rotor, (b) One rotation of generator.....221
Figure 5.12: High speed shaft torque difference signal in time domain for, (a) One rotation of rotor, (b) One rotation of generator.....222
Figure 5.13: Healthy indicator variation with fault level for the high-speed shaft torque response difference signal, (a) RMS, (b)peak to peak, (c) Crest Factor, (d) Standard Deviation 223
Figure 6.1: Health indicators of input shaft torque response spectrum in time domain. The indicators are (a) Peak to peak, (b) Crest Factor, (c) Kurtosis, (d) Shape Factor, (e)Energy Operator, (f) CAL 4, (e) Clearance Factor, (f) Impulse Indicator 228
Figure 6.2: Plot of fundamental frequency amplitude percentage deviation for different crack severity levels and the curve fit details. 229
Figure 6.3: Plot of second natural frequency amplitude percentage deviation for different crack severity levels and the curve fit details. 229
Figure 6.4: Difference torque health indicators such as rms, peak to peak and standard deviation for (a) Input shaft, (b) Output shaft 231

Figure 6.5: Plot of peak to peak and crest factor of output shaft difference torque signal for different crack fault severities 233
Figure 6.6: Health indicators in time domain for hybrid fault with a broken tooth and cracked tooth, which are (a) rms, (b) peak to peak, (c) crest factor, (d) standard deviation, (e) kurtosis, (f) shape factor, (g) energy operator, (h) CAL4, (i) clearance factor, (j) impulse indicator 235
Figure 6.7: Plot of modified side band energy ratio (MSER) and correlation coefficient of the residual signal (CCR) due to hybrid fault of missing tooth and cracked tooth on the sun gear on planetary gearbox 236
Figure 6.8: Distribution of torque data for healthy and 40% crack on pinion teeth of a parallel axis gear box. 237
Figure 6.9: Variation of CCS with increase in crack severity levels 238
Figure 6.10: Variation of CCF with increase in crack severity levels 239
Figure 6.11: Variation of CCS, CCF and CCSF with increase in crack severity levels 241

List of Tables

Table 1.1: Type of gears, specialities, and limitations 3
Table 2.1: Fault characteristic frequencies of planetary gearbox components [52][54]..32
Table 2.2: Summary of the HIs used for diagnosis of various types of gear failure modes 50
Table 3.1: Tooth compliance terms for pinion and wheel in double pair tooth contact ..77
Table 3.2: Gear Parameter Details taken from [102].....102
Table 3.3: Gear Parameter for generating Hybrid Faults..... 111
Table 4.1: Main parameters for the parallel axis gear system model. 128
Table 4.2: Main parameters for the planetary gear system 192
Table 4.3: Physical parameters of planetary gear set 197
Table 5.1: Gear Specifications and Transmission Ratios for Wind Turbine Gearbox Stages.....210
Table 5.2: Parameters from wind turbine power plant dynamic modelling 214
Table 5.3: Natural frequencies and gear mesh frequencies of the wind turbine system215

List of Abbreviations

AGMA	American Gear Manufacturer's Association
AM	Amplitude Modulation
ASM	American Society of Metals
bps	Basis points
CBM	Condition-Based Maintenance
CCR	Correlation Coefficient of Residual signal
CCF	Correlation Coefficient of Fourth moment
CCS	Correlation Coefficient of Second moment
CCSF	Correlation Coefficient of Second and Fourth moment
CF	Crest Factor
DOF	Degrees of Freedom
EO	Energy Operator
FFT	Fast Fourier Transform
FM	Frequency Modulation
FT	Fourier Transform
FW	Face-width of Gear
GMF	Gear-Mesh Frequency (alternate symbol)
HI	Health Indicator
HPF	High-Pass Filter
HSS	High-Speed Shaft
ISS	Intermediate-Speed Shaft
LPF	Low-Pass Filter

LSS	Low-Speed Shaft
MSER	Modified Sideband Energy Ratio
NREL	National Renewable Energy Laboratory
RMS	Root-Mean-Square
RMSDS	RMS of Difference Signal
RMSE	Root-Mean-Square Error
SBR	Side-Band Ratio
SK	Spectral Kurtosis
SR	Stochastic Resonance
STD	Standard Deviation
STFT	Short-Time Fourier Transform
SVM	Support Vector Machine
TEO	Teager Energy Operator
TH	Tooth Height
TSA	Time Synchronous Averaging
TVMS	Time-Varying Mesh Stiffness
WT	Wavelet Transform
WVD	Wigner–Ville Distribution

List of Nomenclature

E	Modulus of Elasticity
$f_{carrier}$	Rotational Frequency of the Planet Carrier
f_{mesh}	Gear-Mesh Frequency
f_{sun}	Rotational Frequency of Sun Gear
G	Modulus of Rigidity
K_t	Equivalent Gear-Mesh Stiffness
k_a	Axial-compression stiffness of gear tooth
k_b	Bending stiffness of gear tooth
k_h	Hertzian contact stiffness
k_s	Shear stiffness of gear tooth
L	Face width of gear
m	Module of gear
N	Number of Planet Pinions
R_b	Base-circle radius of gear
T_{in}	Input-Shaft Torque
T_{out}	Output-Shaft Torque
Z_1	Number of teeth on Pinion
Z_2	Number of teeth on Gear
Z_p	Number of teeth on Planet Gear
Z_r	Number of teeth on Ring Gear
Z_s	Number of teeth on Sun Gear
α_0	Standard Pressure Angle
α_1	Pressure Angle at Contact Point

$\boldsymbol{\alpha_2}$	Half-tooth Angle
$\boldsymbol{d_h}$	Tooth Height
$\boldsymbol{h_w}$	Wear Depth
$\boldsymbol{\nu}$	Poisson's Ratio
$\boldsymbol{\nu_c}$	Crack Angle